# Switching transient induced skin effect in Packet Energy Transfer systems

1st Tamal Sarkar
*Engineering Research*
*VoltServer, Inc.*
East Greenwich, RI, USA
tamal.sarkar@voltserver.com

2nd Jonathan Casey
*Engineering Research*
*VoltServer, Inc.*
East Greenwich, RI, USA
jonathan.casey@voltserver.com

***Abstract*—In this article, the electromagnetic analysis of skin effect during switching transients and faults in transmission cables used in Packet Energy Transfer (PET) systems is investigated. The study covers the electromagnetic diffusion of current density during switching transients in high frequency switched-mode power supplies (SMPS). The mathematical model for such electromagnetic phenomena are discussed and simulation models are developed to illustrate the transition process. The radial current density distribution inside conductor is studied and time domain analysis of the cable resistance and power loss is analyzed. The dynamics of temporal change in total current and effective resistance that account for the power loss during switching transients are also discussed.**

***Index Terms*—Skin Effect, Packet Energy Transfer, Pulsed DC, Current Density Distribution**

## I. Introduction

The ever-increasing range of power electronic applications have added new areas like Electric vehicle (EV) charging [1]–[3], renewable energy conversion, industrial processes and High Voltage DC (HVDC) power transmission [4]–[7] over the last couple of decades. In recent years, fault management has been a major concern for different power systems and many research studies have been conducted and different schemes have been proposed to manage the faults [8]- [9]. Modeling transient properties at normal operating conditions and in the event of fault requires component level studies [10] on switching devices for developing efficient fault detection methods. Fault Managed Power (FMP) Systems are a new class of electrical distribution methodology adopted by the 2023 National Electric Code termed as 'Class 4 power systems'. FMP systems offer inherent safety protection against shock and fire by limiting the charge and energy provided to a fault. One way this is accomplished is by transferring electrical energy in a brief, discreet current pulse of less than a few milliseconds followed by a smaller period where the transmission lines are isolated and analyzed for loss of electrical energy between a transmitter and receiver. After each pulse, the transmission line between a transmitter and receiver device is electrically isolated and analyzed to determine if energy is being lost – for example because a person is touching the power lines, or the lines are shorted. If the transfer of the energy was successful, another pulse is sent, otherwise the lines remain de-energized. This transmission protocol can be referred to as Packet Energy Transfer (PET). PET protects against all the faults found in traditional AC or DC distribution systems, including Arc Fault, Ground Fault and Over-current faults plus two additional faults that traditional distribution systems have not addressed—a line-to-line touch fault and high resistance in-line fault. PET is unique in its ability to detect a poor connection or otherwise abnormally high resistance in the transmission lines, known to the industry as a resistive fault. Resistive faults have been identified as the largest cause of fatalities in residential home electrical fires [11]–[13].

To detect a resistive fault under a wide array of operating conditions a PET system must create an accurate model of the transmission line parameters in real time without reliance on expected values that come with proper installation practices (that are subject to human error). Moreover, a calculation of the series resistance of the transmission lines is subject to the influence of skin effect in systems with pulsed input. The sharp edges of PET current pulses have high frequency current components that migrate towards the periphery on the wire cross-section also known as 'skin effect'. Most of the available literature and research are on power electronic circuit design and control of the system, along with the focus in electromagnetic interference issues [14] or skin effects in AC circuits [15]–[17]. While all these topics are highly important to develop circuits and systems, the transient skin effects in pulsed DC circuits are mostly ignored [18]. Skin effect, if not accounted for, can lessen the accuracy of PET fault detection in larger wire diameters.

This study investigates the dynamic change in resistance of the circuit during switching transients in the PET systems due to the skin effect and its impact on the overall system response in power electronic circuits using 2D FEA techniques for current distribution simulation in cable. In section II, the conventional approach for skin effect and mathematical model for pulsed DC system is discussed. In the following section, the simulation models and results for current density distribution in cylindrical conductors are illustrated along with the dynamic resistance during the switching transients is derived. Finally, the findings of the study and future scope of the work is summarized in section IV.

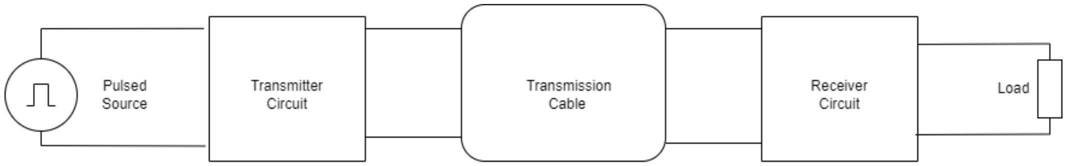


Fig. 1: Basic block diagram of FMP systems

## II. Methodology

In simplified form, the general structure for most FMP systems including PET follows the model depicted in Fig. 1. The converter circuits and transmission cable in such systems are subjected to switching between two or more different voltage states at different frequencies based on the application that causes changes in current distribution in the transmission line. This phenomenon gives rise to transient skin effect in the system. The change in overall cable resistance varies with the current profile and it has significant impact on the transient wave formation.

Different approaches have been made to model and analyze such effect so far [19], [20] but followed the traditional frequency domain approach. Conventional steady state AC skin effect is analyzed using the Maxwell's equation in time harmonic version where time derivatives are replaced with $j\omega$ and results in Bessel's equation. The typical solution of such equation generates the AC skin depth,

$$\delta_{AC} = \sqrt{\frac{2\rho}{\omega\mu}} \tag{1}$$

This equation describes the penetration depth, $\delta$, of the current distribution from the conductor surface for continuous steady-state AC operation at high frequency ($\omega$), which depends on the certain conductor material properties like specific resistance $\rho$ and permeability $\mu$.

When considering the transient regime in PET systems, which occurs in the event of 'turn on' or 'turn off' and in fault conditions, the traditional steady state AC approach fails to explain the dynamics in current distribution. In practice, during turn on or turn off, the transmission line experiences a rise (linear/exponential) or fall in the electromagnetic field that induces current in the cable. This rise or fall can be compared to an injection or removal of a step function in the system with finite rise or fall time (typically $< 100nS$). In typical power electronic devices, it may not have a noteworthy effect in high frequency applications with transient periods shorter than $1\mu S$ but it can have a significant impact if the switching is performed with a long transmission line in a slower switching frequency applications.

The internal transient response during the start or end of each pulse generates different ranges of frequencies in the system response. This process, in turn, changes the conductor resistance from a steady DC parameter to a variable resistive parameter with the added transient resistance due to the skin effect. The impact of such frequency on the transmission line resistance is described in detail by Simon Ramo [21].

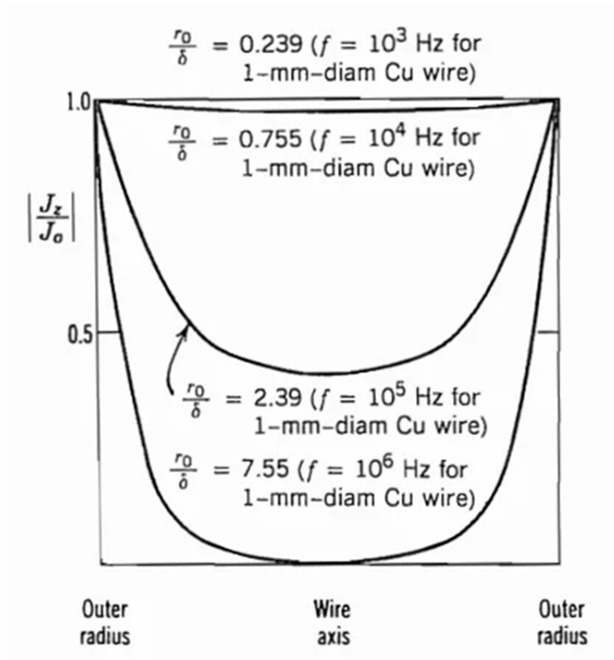


Fig. 2: Normalized magnitude of the current distribution in cylindrical wire [21]

Fig. 2 from [21] shows the normalized magnitude of the current distribution ($|J_z/J_0|$) across the cross-section of a 1-mm-diameter copper round wire at four different frequencies. In Fig. 2, $r_0$ refers to the wire radius and $\delta$ as the skin depth. With the increase in frequency, the skin depth becomes smaller which essentially raises the conductor resistance as the effective cross-section area gets smaller. Due to the nature of reflections in a temporarily isolated conductor during turn on and turn off phases, the transmission line experiences high frequency oscillation that causes the effective resistance to vary during the time period, and with a repeating sequence of pulses, the effective resistance becomes a time varying function.

The electromagnetic diffusion equation governs the current distribution inside a conductor. The current density in the cross section of a cylindrical conductor can be described using Maxwell's curl equations in polar coordinates:

$$\frac{1}{r}\frac{\partial}{\partial r}\left(r\frac{\partial J}{\partial r}\right) + \frac{1}{r^2}\frac{\partial^2 J}{\partial \theta^2} = \sigma\mu\frac{\partial J}{\partial t} \tag{2}$$

This is a form of the diffusion equation that describes the current density, $J$ inside a cylindrical solid core conductor with a radius, $r$ and rotational angle, $\theta$. Here, $\sigma$ and $\mu$ represents the electrical conductivity and permeability of the conductor material. The general solution to the above equation can be derived as:

$$J(r,\theta,t) = \sum_{m=-\infty}^{\infty} \int_{0}^{\infty} \left[E_m I_0(\lambda r) + F_m K_0(\lambda r)\right] \times \left[A_m e^{im\theta} + B_m e^{-im\theta}\right] C e^{-\frac{\lambda^2}{\sigma\mu} t}\, d\lambda \tag{3}$$

The general solution involves the Bessel's function of the first $I_0(\lambda r)$ and the second kind $K_0(\lambda r)$ and can be expressed as the sum of an infinite series with sinusoidal terms. The coefficients $E_m, F_m, A_m, B_m, C$ and $D$ along with constant $\lambda$ can be determined based on the case-specific boundary conditions with numerical analysis. The mathematical process of determining coefficients can be found in different literature available. The process used here followed is described by J. D. Jackson [22].

At the start of the transition during turn on, the current is mostly distributed in the surface of the conductor, similar to the high frequency AC skin effect models, but as the transition continues to reach its saturation, the current is diffused inside the core of the cable and ends up as a uniform distribution across the cross section of the cable that refers to the DC distribution of the current. The total current can be calculated using following equation:

$$I_{\text{total}}(t) = \iint J \cdot dS \tag{4}$$

Here, the total current is integrated from the current distribution over the total cross-section surface of the cable. This change in the penetration depth of current induces the skin effect and in turn there is a dynamic change in total resistance of the transmission line. In this way, instead of a frequency dependent parameter, the resistance during switching transients becomes a temporal function that is responsible for the switching power loss in a transient regime. As the rate of current diffusion in the cable depends on material properties as well as on system configuration, it is convenient to use the current density and total current during transients for calculating the power loss in the system than to formulate temporal equations for the dynamic resistance. Additionally, an approximation for the total power loss can be developed using summation of losses from each harmonic of the input pulse train [23].

## III. Results & Discussion

The current distribution model described in the previous section is simulated using MATLAB and Simulink. To demonstrate, a 12 AWG (diameter 2 mm) isotropic cable is subjected to a pulse current input of 3A with 75 percent duty cycle to a resistive load. For simplicity, the material properties such as electrical conductivity and permeability are assumed to be consistent over the cross section of the cable. The cable parameters and system parameters (i.e. current and voltage profile) used in the simulation model are real-world test data obtained from VoltServer, Inc.'s testing lab.

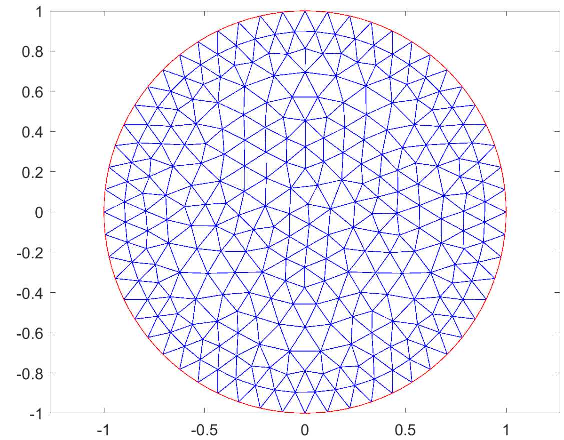


Fig. 3: Cable Cross-section Meshgrid

For the 2D finite element analysis, the MATLAB PDE Modeler App was used to generate the current distribution model. The results are further validated by numerical modeling using the Crank-Nicolson method [24]. Fig. 3 shows the meshgrid formulation of the cable cross-section used for the experiment. The total simulation time is set to 2ms with a time step of 1 $\mu s$ for high resolution.

Fig. 4 illustrates the current density at different time steps during the turn on transition. The initial distribution in Fig. 4(a) shows the majority of the charge carriers are flowing through the surface, referring to a very small effective area and high AC resistance. Over the course of the transition shown in Fig. 4(b) and Fig. 4(c), the current inside the conductor continues to diffuse towards the center which corresponds to an increasing effective area in the cable. The final part shown in Fig. 4(d), depicts the uniform distribution of current over the cross section of the cable that occurs when the transition is complete and the current level reaches it's saturation i.e. DC steady state.

The transition takes place on the order of hundreds of microseconds and responds to the system during switching. A similar but reverse process can be obtained from the turn-off stage of the switching. In this way, during switching, the effective resistance becomes a temporal function and contributes to the switching loss. The total current is obtained from integrating each time step using equation 4 for a sanity check and plotted in Fig. 5.

The dynamic resistance, $R_{(dynamic)}$ is a temporal function during the switching transients and can be defined as:

$$R_{dynamic}(t) = R_{dc} + [V_{applied}(t)/I_{\text{line}}(t)] \tag{5}$$

From the dynamic resistance profile, the in-line power loss can also be calculated in a more accurate manner. The simulated results are validated using analytical solutions discussed in the methodology section. For modeling the packet energy transfer systems more precisely, the discussed method serves

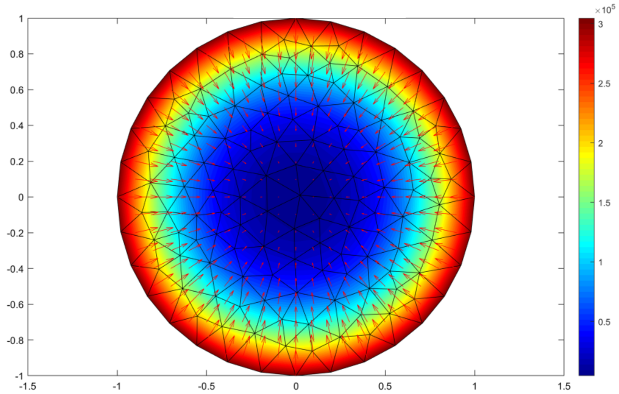


(a) Current Density at $5\mu s$

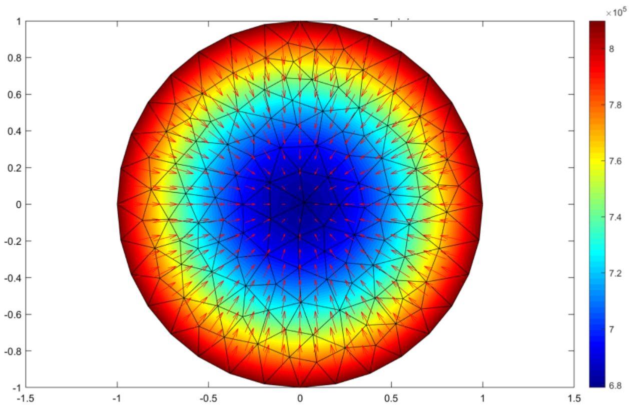


(b) Current Density at $100\mu s$

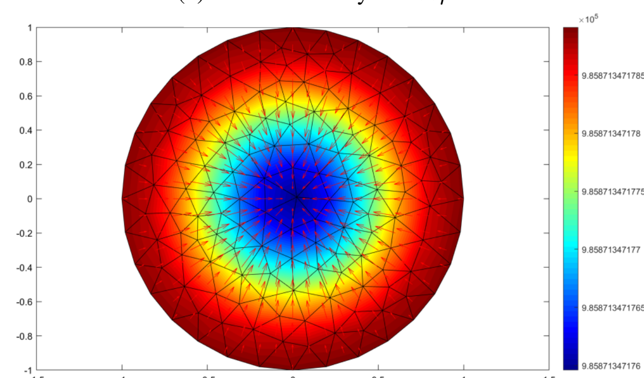

(c) Current Density at $150\mu s$

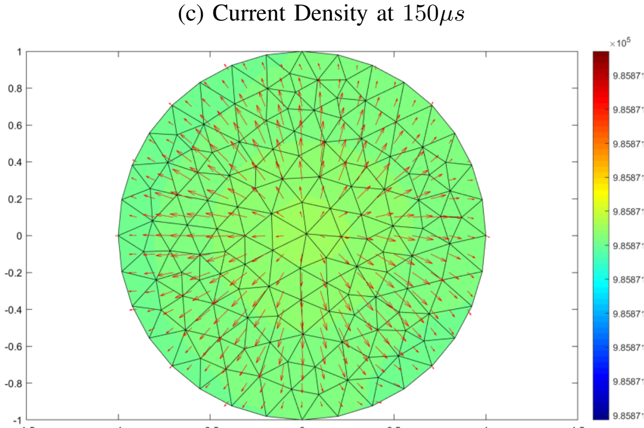

(d) Current Density at $295\mu s$

Fig. 4: Current Distribution in cable cross-section at different time-steps

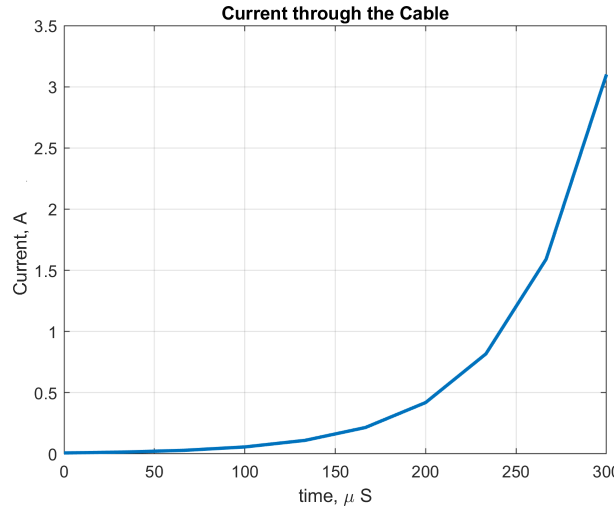


Fig. 5: Total current in the conductor during Turn-On Transient

as a crucial piece for detection and mitigation of in-line high resistance faults.

## IV. Conclusion

The time-domain electromagnetic analysis of the transient skin effect is investigated in this paper. The electromagnetic diffusion of current governed by Maxwell's equations leads toward temporal change in cable and system resistance and contributes to the power loss and predictive analysis of PET power electronic circuits in the events of switching and faults. This study is crucial for developing models and safety algorithms for PET systems such as fault managed power. For improving system performance and reliability, modeling and simulating accurate system response to the component level that incorporates transient skin effects is much needed. In the future, along with the current distribution analysis, the potential distribution along the conductor can be used for effective power calculation and analysis for different ranges and types of transmission wires and cables. Non-homogeneous and more complicated structures of cables subjected to various pulse trains will also be considered.

## References

[1] R. Bosshard and J. W. Kolar, "Inductive power transfer for electric vehicle charging: Technical challenges and tradeoffs," in IEEE Power Electronics Magazine, vol. 3, no. 3, pp. 22-30, Sept. 2016, doi: 10.1109/MPEL.2016.2583839.

[2] H. K. Bai et al., "Charging Electric Vehicle Batteries: Wired and Wireless Power Transfer: Exploring EV charging technologies," in IEEE Power Electronics Magazine, vol. 9, no. 2, pp. 14-29, June 2022, doi: 10.1109/MPEL.2022.3173543.

[3] S. Habib et al., "Contemporary trends in power electronics converters for charging solutions of electric vehicles," in CSEE Journal of Power and Energy Systems, vol. 6, no. 4, pp. 911-929, Dec. 2020, doi: 10.17775/CSEEJPES.2019.02700.

[4] Y. Chen, Z. Li, S. Zhao, X. Wei and Y. Kang, "Design and Implementation of a Modular Multilevel Converter With Hierarchical Redundancy Ability for Electric Ship MVDC System," in IEEE Journal of Emerging and Selected Topics in Power Electronics, vol. 5, no. 1, pp. 189-202, March 2017, doi: 10.1109/JESTPE.2016.2632858.

[5] H. Liu and J. Sun, "Voltage Stability and Control of Offshore Wind Farms With AC Collection and HVDC Transmission," in IEEE Journal of Emerging and Selected Topics in Power Electronics, vol. 2, no. 4, pp. 1181-1189, Dec. 2014, doi: 10.1109/JESTPE.2014.2361290.

[6] X. Luo, S. Niu, S. L. Ho and W. N. Fu, "A Design Method of Magnetically Resonanting Wireless Power Delivery Systems for Bio-Implantable Devices," in IEEE Transactions on Magnetics, vol. 47, no. 10, pp. 3833-3836, Oct. 2011, doi: 10.1109/TMAG.2011.2148108.

[7] C. W. Gellings, M. Samotyj and B. Howe, "The future's smart delivery system [electric power supply]," in IEEE Power and Energy Magazine, vol. 2, no. 5, pp. 40-48, Sept.-Oct. 2004, doi: 10.1109/MPAE.2004.1338121.

[8] K. Satpathi, A. Ukil, S. S. Nag, J. Pou and M. A. Zagrodnik, "DC Marine Power System: Transient Behavior and Fault Management Aspects," in IEEE Transactions on Industrial Informatics, vol. 15, no. 4, pp. 1911-1925, April 2019, doi: 10.1109/TII.2018.2864598.

[9] Z. Ali et al., "Fault Management in DC Microgrids: A Review of Challenges, Countermeasures, and Future Research Trends," in IEEE Access, vol. 9, pp. 128032-128054, 2021, doi: 10.1109/ACCESS.2021.3112383.

[10] T. Sarkar, J. Casey and N. Lutz, "Modeling MOSFETs for fault-managed power systems: a transient analysis based on capacitance dynamics," 2023 IEEE Energy Conversion Congress and Exposition (ECCE), Nashville, TN, USA, 2023, pp. 6156-6160, doi: 10.1109/ECCE53617.2023.10362333.

[11] S. Montgomery, "Required Technology to Prevent Electrical Fire Ignition", IAEI Magazine, 2011. url: https://iaeimagazine.org/2011/september2011/required-technology-to-prevent-electrical-fire-ignitions/, url date: 2023-12-09.

[12] "Home Electrical Fires", Electrical Safety Foundation, 2023. url: https://www.esfi.org/home-electrical-fires, url date: 2023-12-09.

[13] V. Babrauskas, "Smoking Out the Main Causes of Electrical Fires", EC&M, 2021. url: https://www.ecmweb.com/safety/article/21178987/smoking-out-the-main-causes-of-electrical-fires, url date: 2023-12-09.

[14] A. Dutta and S. S. Ang, "Effects of parasitic parameters on electromagnetic interference of power electronic modules," 2017 IEEE Applied Power Electronics Conference and Exposition (APEC), Tampa, FL, USA, 2017, pp. 2706-2710, doi: 10.1109/APEC.2017.7931081.

[15] K. -T. Kim et al., "Skin Effect-Related AC Resistance Study in Macroscopic Scale Carbon Nanotube Yarn Applicable to High-Power Converter," in IEEE Transactions on Nanotechnology, vol. 20, pp. 417-424, 2021, doi: 10.1109/TNANO.2021.3076472.

[16] J. R. González-Teodoro, V. Kindl, E. Romero-Cadaval and R. Asensi, "Analysis of Skin Effect in Single Wire Resistance by Finite Element Methods," 2020 IEEE 14th International Conference on Compatibility, Power Electronics and Power Engineering (CPE-POWERENG), Setubal, Portugal, 2020, pp. 19-23, doi: 10.1109/CPE-POWERENG48600.2020.9161540.

[17] N. Idir, Y. Weens and J. -J. Franchaud, "Skin effect and dielectric loss models of power cables," in IEEE Transactions on Dielectrics and Electrical Insulation, vol. 16, no. 1, pp. 147-154, February 2009, doi: 10.1109/TDEI.2009.4784562.

[18] C. Donaghy-Spargo and A. Horsfall, "Transient skin effect in power electronic applications", The Journal of Engineering, vol. 2019, number 17, pp. 3696-3700, doi: 10.1049/joe.2018.8132

[19] S. H. L. Cabral et al., "Practical Aspects of the Skin Effect in Low Frequencies in Rectangular Conductors," in IEEE Access, vol. 9, pp. 49424-49433, 2021, doi: 10.1109/ACCESS.2021.3069821. 54.

[20] T. H. Petersen, K. H. Carpenter and C. M. May, "Comparison of Experimental Measurements of Current Distribution in a Flat Conductor With Simulated Results From the Partial Inductance Method," in IEEE Transactions on Electromagnetic Compatibility, vol. 51, no. 2, pp. 345-350, May 2009, doi: 10.1109/TEMC.2009.2015939.

[21] S. Ramo, J. Whinnery, T. Duzer, "Fields and Waves in Communication Electronics", 3rd Edition, Wiley, March 1994, ISBN: 978-0-471-58551-0.

[22] John David Jackson, "Classical Electrodynamics", 3rd Edition, Wiley, August 1998, ISBN: 978-0471309321.

[23] A. Pokryvailo, "Losses in a conducting cylinder carrying periodic nonsinusoidal current," 2014 IEEE International Power Modulator and High Voltage Conference (IPMHVC), Santa Fe, NM, USA, 2014, pp. 245-248, doi: 10.1109/IPMHVC.2014.72872

[24] Crank, J. and Nicolson, P. (1947) A Practical Method for Numerical Evaluation of Solutions of Partial Differential Equations of the Heat-Conduction Type. Mathematical Proceedings of the Cambridge Philosophical Society, 43, 50-67. https://doi.org/10.1017/S0305004100023197